Available online at www.sciencedirect.com
SCIENCE DIRECT®
Journal of Power Sources 154 (2006) 394–403
JOURNAL OF POWER SOURCES
www.elsevier.com/locate/jpowsour

Dynamic behaviour of SOFC short stacks

Michele Molinelli [a], Diego Larrain [a], Nordahl Autissier [a], Raphaël Ihringer [b], Joseph Sfeir [b], Nicolas Badel [b], Olivier Bucheli [b], Jan Van herle [a,*]

[a] *Laboratory of Industrial Energy Systems (LENI), Faculty of Engineering, Ecole Polytechnique Fédérale de Lausanne (EPFL), CH-1015 Lausanne, Switzerland*
[b] *HTceramix S.A., 18 Avenue des Sports, CH-1400 Yverdon-les-Bains, Switzerland*

Available online 28 November 2005

Abstract

Electrical output behaviour obtained on solid oxide fuel cell stacks, based on planar anode supported cells (50 or 100 cm^2 active area) and metallic interconnects, is reported. Stacks (1–12 cells) have been operated with cathode air and anode hydrogen flows between 750 and 800 °C operating temperature. At first polarisation, an activation phase (increase in power density) is typically observed, ascribed to the cathode but not clarified. Activation may extend over days or weeks. The materials are fairly resistant to thermal cycling. A 1-cell stack cycled five times in 4 days at heating/cooling rates of 100–300 K h^{-1}, showed no accelerated degradation. In a 5-cell stack, open circuit voltage (OCV) of all cells remained constant after three full cycles (800–25 °C). Power output is little affected by air flow but markedly influenced by small fuel flow variation. Fuel utilisation reached 88% in one 5-cell stack test. Performance homogeneity between cells lay at ±4–8% for three different 5- or 6-cell stacks, but was poor for a 12-cell stack with respect to the border cells. Degradation of a 1-cell stack operated for 5500 h showed clear dependence on operating conditions (cell voltage, fuel conversion), believed to be related to anode reoxidation (Ni). A 6-cell stack (50 cm^2 cells) delivering 100 W_{el} at 790 °C (1 kW_{el} L^{-1} or 0.34 W cm^{-2}) went through a fuel supply interruption and a thermal cycle, with one out of the six cells slightly underperforming after these events. This cell was eventually responsible (hot spot) for stack failure.

Keywords: Solid oxide fuel cells; Dynamic behaviour; Cathode activation; Thermal cycling; Degradation

1. Introduction

Planar solid oxide fuel cells (SOFC) are reaching the stage that reasonable durability under steady state operating conditions can be achieved (e.g. <2% degradation/1000 h for several 1000 h [1,2]), when properly addressing microstructural stabilisation especially of the electrodes [3] and minimising interfacial reactions at electrode/electrolyte [4] and electrode/current collector boundaries [5,6]. In addition to steady state durability, the technology also has to cope with transient situations such as start-up/shut-down, conditioning protocols (first operation), thermal cycling or thermal runaway, reforming dynamics, gas supply failures, etc. This is especially true for planar stacks, where different thin ceramic and metal layers with an amount of sealant alternate in a compact volume where reactive gases circulate in a pressure and temperature gradient. Understanding and control of the dynamics of the devices is as much key to successful application as minimal long-term degradation. The present contribution reports on test results obtained on short SOFC stacks of recent design [7] and emphasizes aspects of their transient behaviour.

2. Experimental

The cells supplied by the company HTceramix S.A. are composed of planar, nickel–zirconia anode supported, 200 μm thin cells with a 6 μm zirconia electrolyte, fabricated by tape casting, and a 30 μm perovskite cathode, deposited by screen printing [8]. They are assembled to stacks using 750 μm flat metal interconnect sheets (T-458 from Allegheny Ludlum, United States) and intercalated gas distribution layers (SOFCONNEX^{TM} design [7]), for a repeating unit height below 3 mm. The stack footprint is 8 cm × 8 cm, the cathode active area around 50 cm^2. Manifolding is internal, via feed holes for air and fuel, exiting at opposite edges left unsealed [9]. The assembled stacks, sometimes consisting of a single repeating unit, are compressed (spring-load, usually 0.4 kg cm^{-2}) in a metal housing equipped with feeding tubes and electrical feedthroughs and which fits into a test furnace (Rohde, Germany). They are

* Corresponding author. Tel.: +41 21 693 35 10; fax: +41 21 693 35 02.
E-mail address: jan.vanherle@epfl.ch (J. Van herle).

0378-7753/$ – see front matter © 2005 Published by Elsevier B.V.
doi:10.1016/j.jpowsour.2005.10.040

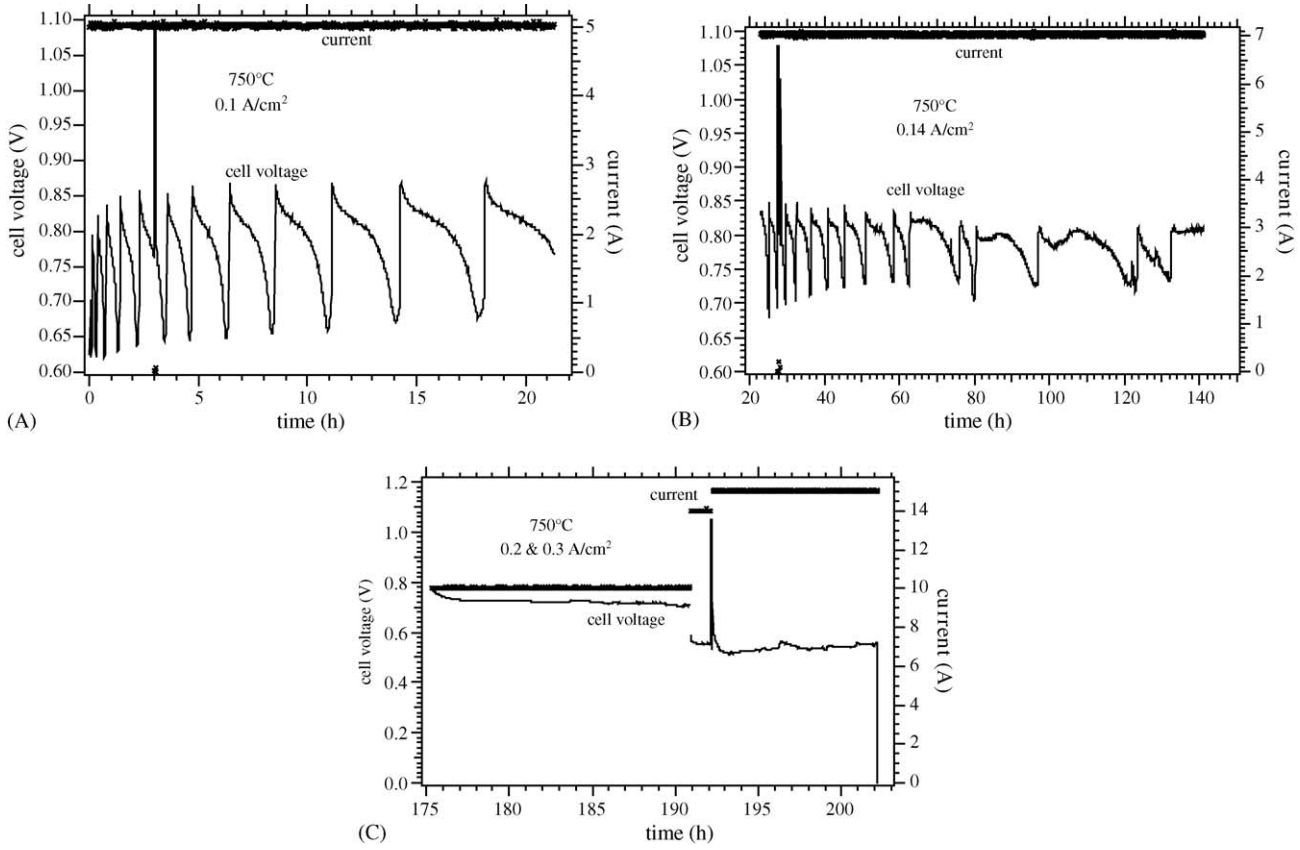

Fig. 1. Cell voltage as a function of time for a 1-cell stack (50 cm^2 active area) at 750 °C polarised galvanostatically, H_2 flow 210 ml min^{-1}, air flow 2 L min^{-1}, displaying oscillating behaviour (A and B), stabilisation and final failure at low voltage (C).

typically heated at 150 K h^{-1} to 750 °C under air flow; at high temperature, argon is flushed to the anode compartments then replaced with hydrogen, usually with and more rarely without humidification (2–3% water vapour, gas washing bottle). Electrical characterisation is performed using an electronic load (60 A, Agilent 6060B) and voltage source (Kepco RCW-350W) in series with the stack elements. Impedance spectroscopy is carried out using equipment from Zahner Elektrik GmbH, Germany. When not specified otherwise below, typical gas flows were of 8 ml min^{-1} cm^{-2} for H_2 and 40 ml min^{-1} cm^{-2} for air, and the furnace temperature 750 °C, leading to local temperatures between 760 and 790 °C depending on gas flows and location of the thermocouples. Voltage, current, temperature and pressure values are monitored on line using data acquisition.

Some of the cells were fabricated to 100 cm^2 active area with a central fuel feed hole and tested as 5-cell stacks in a design employed at Sulzer AG, Switzerland [10], using metal interconnects with channeling structure. Testing conditions were otherwise very similar (800 °C, humidified H_2, air, 0.4 kg cm^{-2} load) to those specified above.

3. Results and discussion

3.1. Cathode activation

With first operation of several short stacks (one to four repeating units), oscillating cell voltage was observed, an example of which is given in Fig. 1. The oscillations are severe (amplitude up to 200 mV, constant current 0.1 A cm^{-2}) and slow (period of 1 h and more). Whether as a function of time or of current density, the amplitude decreases (to less than 100 mV after 50 h, at increased current density of 0.14 A cm^{-2}) and the period increases (Fig. 1A and B), until the oscillation disappears after 1 week. The voltage oscillation was independent of the operating point: when switching the cell to open circuit (OCV) and back to polarised condition (Fig. 1A, 3 h and B, 27 h), the oscillation continued from where it left before the interruption to OCV. This does not support the interpretation that the oscillation would be due to steam accumulation in the anode: after a switch to OCV, one would expect stagnant steam to be purged and thus, upon renewed polarisation, the cell voltage to be higher than before the interruption.

We have observed these oscillations with a cathode type of $LaSrMnO_3$, and only on 50 cm^2 repeating units, not on small single cells (10 cm^2 anode supports, 1 cm^2 cathodes, using Pt and Ni mesh current collectors [8,11]) from otherwise identical making. When replacing the $LaSrMnO_3$ (LSM) cathode with a different material, $LaSrFeO_3$ (LSF), no oscillations occur (Figs. 2 and 3). The oscillation shape displayed in Fig. 1A and B resembles a polarographic half wave [12], as described before for LSM cathodes when strongly polarised and then allowed to relax to a new state [13,14], determined to be related to the Mn^{3+}/Mn^{4+} redox couple present in the material [13,15]. The phenomenon might thus be related to oxygen starvation and cathode reduction in

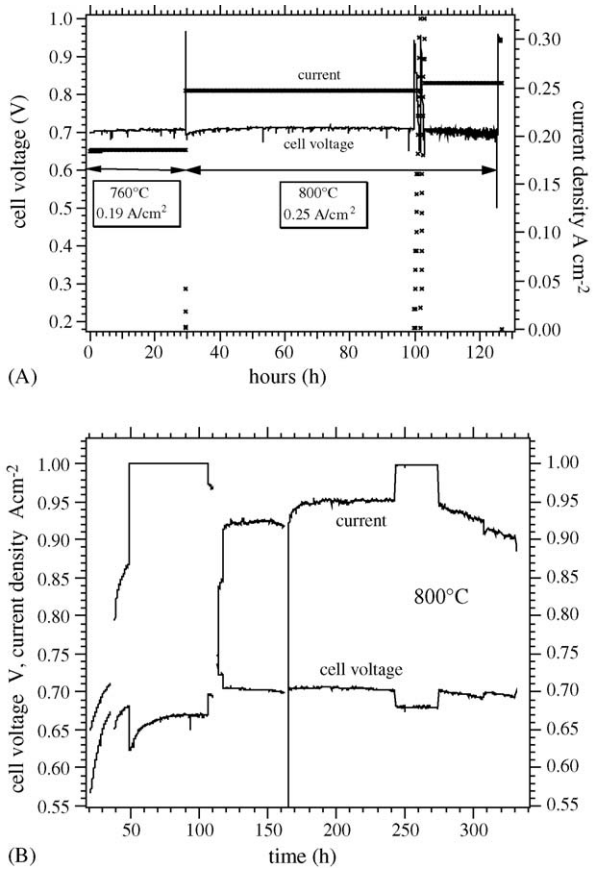

Fig. 2. Cell voltage as a function of time (A) for a 1-cell stack (50 cm^2 active area) at 800 °C polarised galvanostatically, H_2 flow 4.8 ml min^{-1} cm^{-2} (fuel utilisation 40% at 13 A), air flow 30 ml min^{-1} cm^{-2} and (B) for a small single cell (1 cm^2 cathode, Pt and Ni mesh collectors), H_2 flow 140 ml min^{-1}, air flow 280 ml min^{-1}, both displaying performance activation. In (B), decay beyond 280 h was under potentiostatic control (0.7 V), but with some instrumental instability artefact.

poorly air-fed zones of a stack element (not occurring in a small single cell test flown with large air excess), generally due to leaks. Nevertheless, it is not understood or quantifiable at the present time.

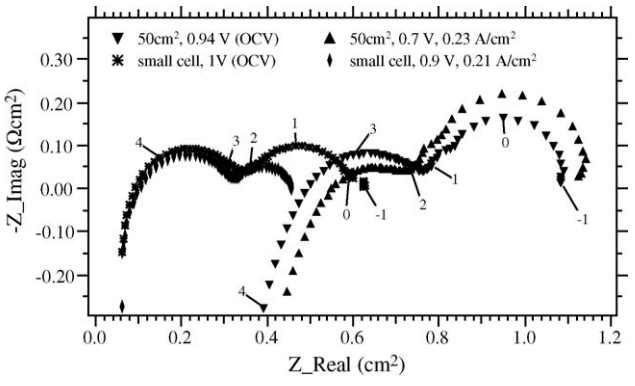

Fig. 3. Impedance spectroscopy result on a small cell (1 cm^2 cathode on 10 cm^2 anode support, with Pt and Ni mesh current collectors) and a 1-cell stack element (50 cm^2 cell with metal interconnects) at similar test temperature (800 °C) and current density (OCV, 0.2 A cm^{-2}) (cf. Fig. 2A and B). Numbers −1 to 4 indicate sweep frequencies in powers of 10 Hz.

Fig. 1C finally illustrates that cell failure occurred (205 h) when at low polarisation voltage (ca. 0.5 V for 15 A or 0.3 A cm^{-2}, fuel utilisation 50%), even though operation then appeared more stable than at higher voltage (0.7 V, 175–190 h in Fig. 1C). This was noted several times (see also Fig. 17), believed to be related to anode limitation and will be discussed further below.

Fig. 2A shows that oscillations were absent when using an LSF cathode with otherwise identical configuration and test conditions. In addition, a small activation of the performance can be seen. Finally, it is noted that termination of this test (125 h) is preceded by small random fluctuations, possible pointing to crack initiation around a hot spot, until cell fracturing: post mortem inspection showed a single crack passing the fuel feed hole. The activation is more clearly observed on a small single cell with noble mesh current collectors (Fig. 2B), where current can be substantially higher and where no overlapping degradation occurs due to the deteriorating metal interconnect contact resistance, which is measured separately and known to take place from the beginning onwards of each test [7].

Activation spreads over roughly 100–200 h (measured repeatedly on several small and large cells) until stabilisation. From the comparison between Fig. 2A (stack element, 50 cm^2) and Fig. 2B (small single cell, 1 cm^2 cathode), measured on identical materials, a performance difference of almost a factor 4 (0.25 A cm^{-2} versus 0.95 A cm^{-2}, both at 0.7 V) is visible. Electrochemical impedance spectroscopy, EIS (Fig. 3), points to the various contributions to this difference. From the measurements is seen that both the ohmic (0.4 Ω cm^2 versus 0.1 Ω cm^2) and the polarisation loss (0.7 Ω cm^2 versus 0.35 Ω cm^2) largely contribute (values given for the spectra taken at similar current density, ca. 0.2 A cm^{-2} in both cases). The increased ohmic loss is due to additional contribution from the metal interconnects and related to contact inhomogeneity for the larger surface (confirmed by independent measurements), the increased polarisation loss to higher local current density and strongly different flow fields between both tests. Closer investigation in this direction, especially of EIS data and using a segmented stack repeating element, was conducted [16]. Fig. 3 also shows that the frequency windows of the two arcs have shifted between both cell cases and that impedance grows with dc-bias for the large cell (concentration limitation) but diminishes with dc-bias for the small cell. For the latter, at high current density (1.6 A cm^{-2}, 0.5 V cell potential), the cell polarisation resistance drops to 0.25 Ω cm^2.

Figs. 4 and 5 show that, by further cathode optimisation, the performance gap between a small single cell (800 °C, 0.9 W cm^{-2}, 0.7 V) and a larger stack element can be reduced (750 °C, 0.42 W cm^{-2}, 0.62 V) to roughly a factor of 2, further confirmed by comparing the EIS results (not shown) and the approximate *I–V* curve slopes for both systems (apparent area specific resistance or asr, in Ω cm^2), relating as 0.25 and 0.54 Ω cm^2, respectively. Again an increase in performance is observed (cathode activation): the increase is limited to only 10% (for 450 h) for the stack element, because of compensation by overlapping decay mechanisms (e.g. the metal interconnect contacts), but is very strong for the small single cell,

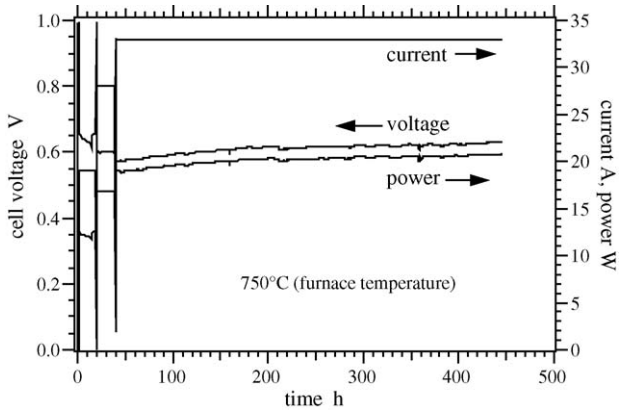

Fig. 4. Voltage and power as a function of time for a 1-cell stack (50 cm^2) at 750 °C furnace temperature (ca. 780 °C local cell temperature) and 33 A (70% fuel conversion, 33% electrical efficiency), H_2 8 ml min^{-1} cm^{-2}, air 50 ml min^{-1} cm^{-2}, showing continuous performance increase.

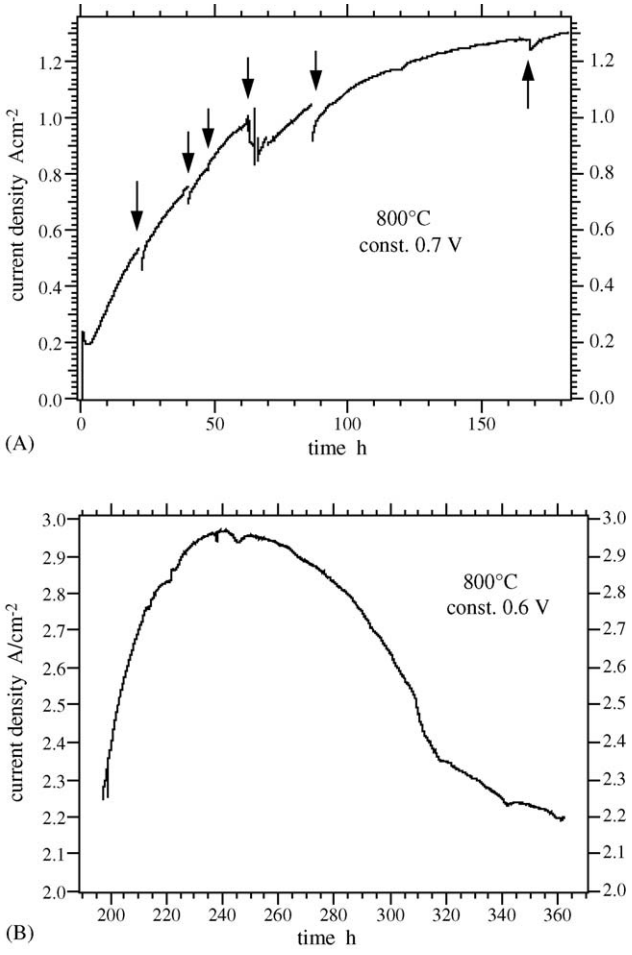

Fig. 5. Current density as a function of time for a small single cell (1 cm^2 cathode) at 800 °C cell temperature and 0.7 V (A), respectively, 0.6 V (B), H_2 120 ml min^{-1}, air 250 ml min^{-1}, showing continuous increase, but strong degradation beyond 3 A cm^{-2}. Arrows in (A) indicate the short interruption of polarisation for recording of *I–V* characteristics.

starting at just 0.2 A cm^{-2} at constant voltage polarisation of 0.7 V and reaching 1.3 A cm^{-2} 180 h later. This marked increase was reported before for LSM by some of the authors [11] and more recently for LSF by Simner et al. [17,18], referred to as "burn-in". The phenomenon is explained as improved electrode/electrolyte adhesion (a current density effect) and reductive redissolution of phases formed during cathode sintering (a voltage effect) [18]. Baumann et al. report an important improvement in $LaSrCoFeO_3$ cathode behaviour, when strongly polarised, due to field-induced surface compositional changes [19]. When taking the cell further to yet higher current density (polarised at 0.6 V; Fig. 5B), a maximum of 3 A cm^{-2} is reached after which performance strongly deteriorates. Post mortem SEM investigation of the sample did not point to direct evidence for this drop: no delamination, interfacial reaction nor significant grain coarsening could be seen. Further examination is ongoing. For stack operation, our numerical modeling shows that maximum local current density (fuel inlet) does not exceed 1.5 A cm^{-2}. It is therefore not an aim to attain long-term stability at 3 A cm^{-2} or more.

3.2. Thermal cycling

Reasonable resistance is observed to temperature cycles, whether intended or unintended (the latter being more likely to happen in real application), as illustrated in Figs. 6 and 7.

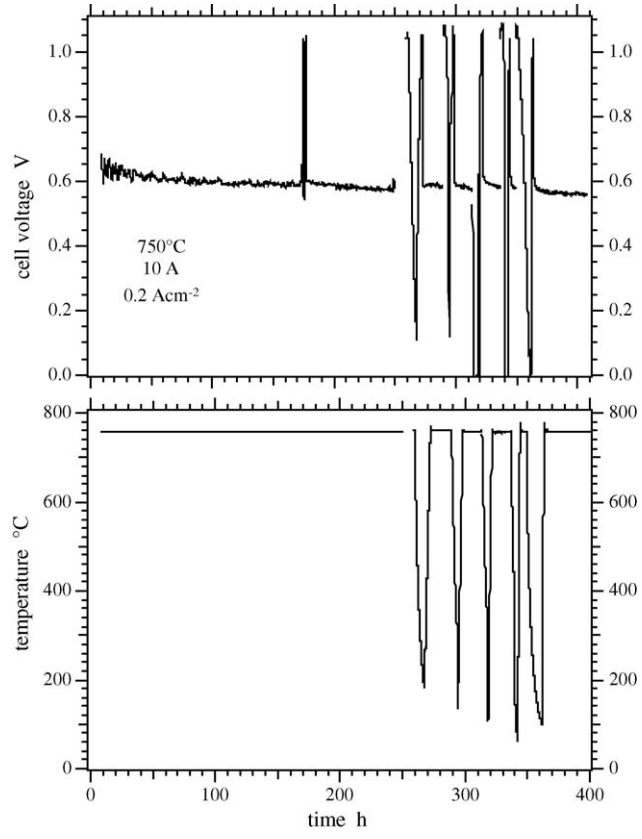

Fig. 6. Voltage and temperature as a function of time for a 1-cell stack (50 cm^2) subjected to five thermal cycles down from 750 °C. H_2 flow of 4 ml min^{-1} cm^{-2}, air flow 20 ml min^{-1} cm^{-2}.

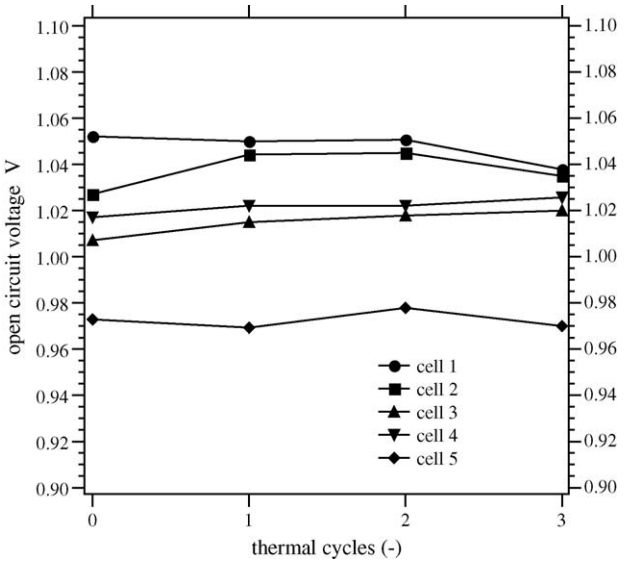

Fig. 7. Open circuit voltage of all cells in a 5-cell stack before and after each of three thermal cycles between 800 and 25 °C.

Fig. 6 shows a 1-cell stack (50 cm^2) operated over 400 h undergoing five cooling/heating ramps between 100–200 and 750 °C in the space of 100 h, i.e. roughly a cycle per day. The cell bore a LSM cathode and displayed initial voltage oscillations edging out after around 100 h (cf. Fig. 1). Fuel conversion on this cell was 35% with a H_2 flow of 4 ml min^{-1} cm^{-2}.

Before each cycle, the cell was left to OCV and cooled down with flowing H_2 and air; after reheat, polarisation (10 A) was reapplied soon after reaching final operating temperature (750 °C). The cooling rate was 120 K h^{-1} for the first three cycles down to 500 °C, then accelerated to 200 K h^{-1}. Initial cooling for cycles 4 and 5 was 200 K h^{-1}, then 250 K h^{-1} for cycle 4 (till 70 °C) and natural cooling in cycle 5 (till 100 °C). Reheat rates were 120, 150 and 200 K h^{-1} for cycles 1, 2 and 3, respectively, and 350 K h^{-1} for cycles 4 and 5. These different ramps, closely following each other, do not appear to affect the single cell stack performance, which picks up the same degradation slope (−10%/1000 h) notable already before cycling.

Thermal cycling was also performed on a 5-cell stack using 100 cm^2 HTceramix circular cells at Sulzer Innotec, at heating/cooling rates of 120 K h^{-1} between 800 and 25 °C. Stability of the open circuit voltage for all cells – variation within 2% (Fig. 7) – demonstrated the electrolyte gas tightness and absence of fissuring.

3.3. Gas flow conditions

Another influence of importance is that of stack performance dependence upon fuel and air flow, pointing both to flow homogeneity between cells in a stack and flow distribution within a repeating unit. The goals are to optimise fuel flow in order to simultaneously satisfy electrical efficiency and power density and to optimise air flow in order to reach sufficient cell cooling but limit air pressure drop in a stack made as compact as possible. Fig. 8 shows results for a 5-cell stack (100 cm^2 cells, Sulzer test).

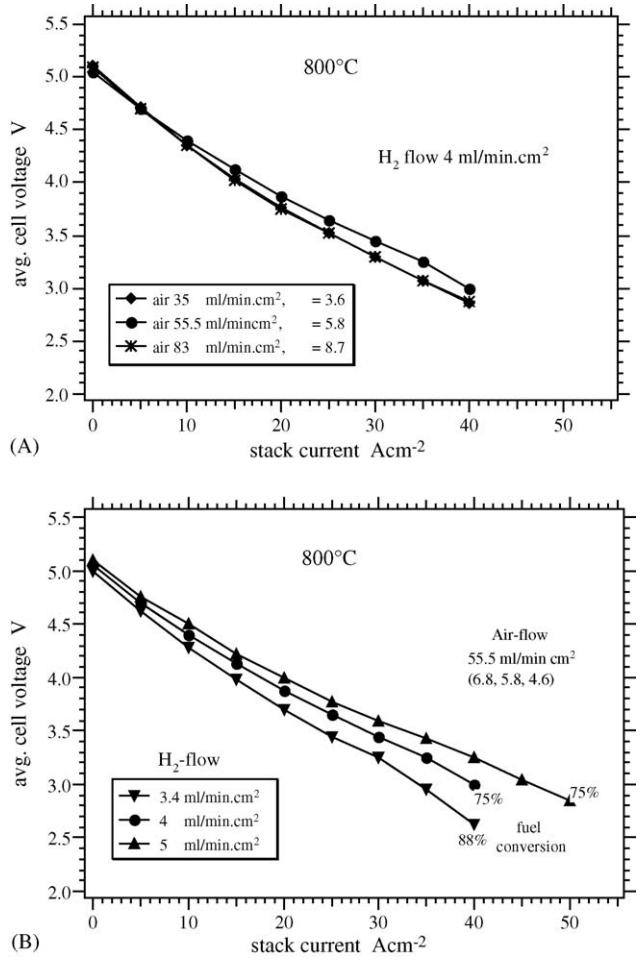

Fig. 8. Performance dependence of 5-cell stack (100 cm^2 cells) on air flow (A) and fuel flow (B) variation at 800 °C.

Air flow dependence (Fig. 8A) varied between 35 and 83 ml min^{-1} cm^{-2} at constant H_2 flow to the anodes (4 ml min^{-1} cm^{-2}), corresponding to a λ-variation between 3.6 and 8.7, showed marginal differences (5%). However, the dependence was significant even for small H_2 flow variation (Fig. 8B) between 3.4 and 5 ml min^{-1} cm^{-2}. For the smallest flow, fuel utilisation reached 88% and electrical efficiency (LHV) of 37%.

Performance homogeneity between the cells (not shown) was satisfactory: for the 5-cell stack reported in Fig. 8 the spread was 5.6%, for a second 5-cell stack tested in identical conditions this spread was 8.2%. For a 6-cell stack mounted and tested in the HTceramix SOFCONNEX™ design (see further below Fig. 14), the cell-to-cell performance spread was 3.6%.

However, an earlier test on a 12-cell stack (50 cm^2 cells) indicated severely inhomogeneous performance distributions.

For this stack, Fig. 9 displays the voltage values per cell between OCV and 10 A stack current (0.2 A cm^{-2}) in steps of 1 A. Low overall OCV (11.2 V for the stack or 0.93 V cell average) points to important gas leakage from the beginning. The border cells are the coldest in the stack and under higher constraint as center cells can rely on several distribution layers above and below to better absorb constraint differences. This appears in Fig. 9A, where the top and bottom cells (1 and 12) quickly

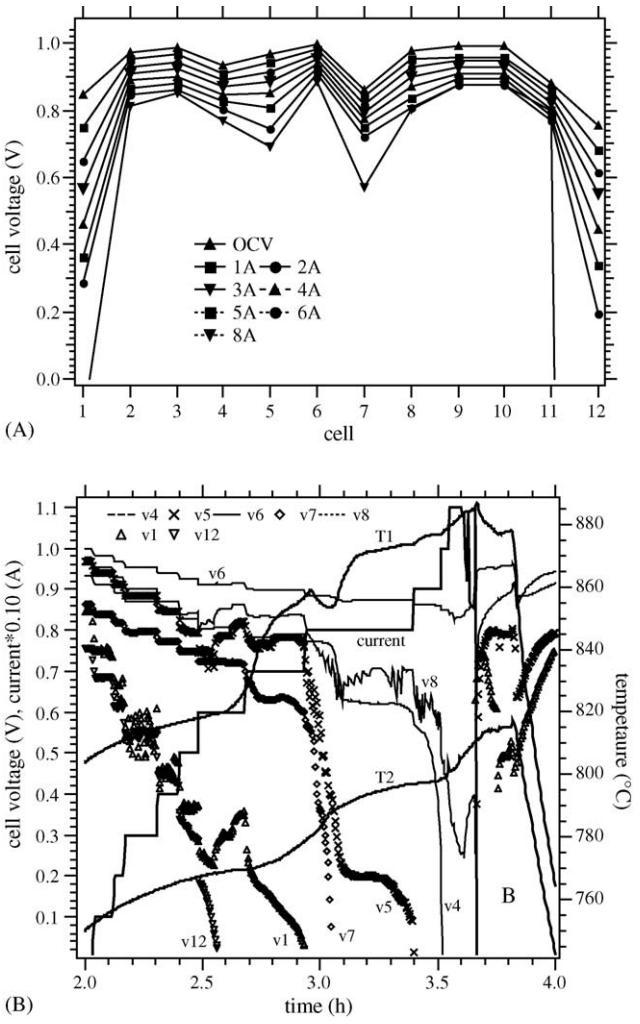

Fig. 9. Performance of early 12-cell stack: (A) indicating leakage and low output of border cells, and (B) successive failure of cells 12, 1, 7, 5, 4 paired with temperature rise due to combustion. The remaining cells not plotted (2, 3, 9, 10, 11) behaved correctly and closely like cell 6.

reach performance limits (below 0.3 V at 6 A) when the other cells maintain average cell voltage above 0.8 V. Cells 5 and 7 are next to follow (at 8 A) in limiting the stack output. In Fig. 9B, one notices the increase in temperature after failure of cell 1 at first, then after failure of cells 5 and 7, due to the creation of direct combustion zones in the stack. An important temperature shift exists between air inlet (T_1) and H_2 outlet (T_2), arising from insufficiently preheated air flow and from thermal runaway. Post mortem inspection revealed that cells 1 and 12 used an active surface of only 40 and 20%, respectively (due to insufficient fuel feed or a severe leak) and that cells 5 and 7 showed multiple cracks, related probably more to inferior mechanical integrity or to an assembly fault than to their position in the stack. The degradation on cells 5 and 7 appeared to quickly affect the neighbouring cells 4 and 8, visible in Fig. 9A and more clearly in Fig. 9B, plotted as a function of time. Surprisingly, the intercalated neighbour cell 6 remains unaffected, confirmed from post mortem inspection (Fig. 10). The same applied to the remaining cells 3, 8–11. It is therefore an uneasy task to try and predict the behaviour of one cell on others in the stack as several parameters

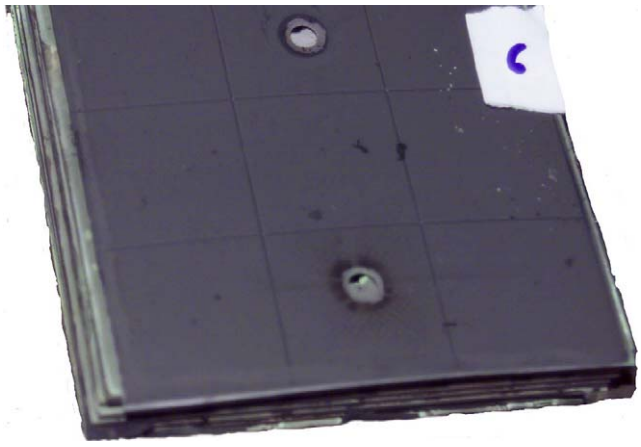

Fig. 10. Post-test aspect of cell number 6 of the 12-cell stack, remaining intact despite failure of the neighbouring cells 5 and 7.

are still ill-controlled (e.g. invisible mechanical defects in a cell prior to testing, minor misalignments during stack assembly and sealing). Ni-based anode supported cells are especially sensitive to variable pO_2 atmospheres, where fluctuations between reducing and oxidising conditions lead to contraction–expansion and soon to cell cracks. This is most critical at the cell edges where, moreover, temperature is higher due to post-combustion.

In order to more closely investigate the effect of flow field, experiments were performed on a segmented repeating unit, allowing to measure localised current density (eight segments with surfaces between 6 and 9 cm^2 each). Detailed results will be reported separately. In one particular test, every segment was individually polarised to around 0.4 A cm^{-2}, after which current was interrupted and the segment voltage relaxation to OCV monitored with time. Results for selected segments are displayed in Fig. 11. It is observed that the fuel entry segment immediately restores to OCV as expected, that a centre and a corner segment (towards the fuel exit) take 2–3 min, and finally that a corner segment next to fuel entry requires up to 10 min to restore original OCV. Whether steam evacuation or

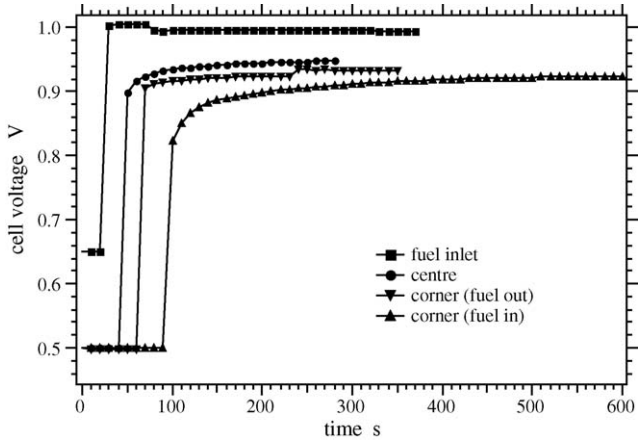

Fig. 11. Local cell voltage as a function of time, for galvanically separated zones of a segmented stack repeating unit, after current interruption from ca. 0.4 A cm^{-2} per segment, 800 °C, H_2 flow 2.5 ml min^{-1} cm^{-2}, air flow 20 ml min^{-1} cm^{-2}.

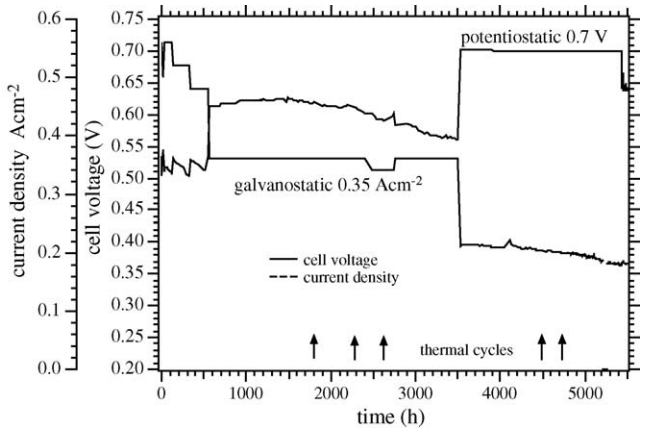

Fig. 12. Voltage and current as a function of time for a 1-cell stack, 750 °C, H_2 flow 8 ml min^{-1} cm^{-2}, air flow 40 ml min^{-1} cm^{-2}, showing degradation dependence upon operating point. Small arrows indicate thermal cycles.

air supply is dominant remains to be determined. The relaxation curves can be approximated by a double exponential (1 for each process), with time constants of 10 and 80 s, respectively, for the centre and exit corner segments, but 16 and 160 s for the inlet corner segment. This type of experiments, paired with extensive modeling [9,20,21,22], allow us to now design a different cell configuration, with improved flow field and fuel conversion.

3.4. Long-term degradation

Degradation in electrical output is explained by a complex superposition of a variety of processes with different time constants. Apart from inherent materials control, the operating conditions will also influence the durability. Performance loss of a 1-cell stack operated for 5500 h showed clear dependence on cell voltage (Fig. 12). At successive current densities of 0.56, 0.52 and 0.48 A cm^{-2} (first 500 h, fuel utilisation 45–50%), cell voltage was ca. 0.52 V and power loss severe (-0.1 mV h^{-1} or -20%/1000 h). At reduced current of 0.36 A cm^{-2} (fuel utilisation 35%) and cell voltage around 0.6 V, a reactivation was observed (+2% in 1000 h) before renewed but lessened degradation set in (-5%/1000 h over 2000 h). At the final condition of 0.7 V constant voltage (ca. 0.2 A cm^{-2}, fuel utilisation 20%), degradation was maintained at first to -5%/1000 h for 1000 h, then accelerated to -10%/1000 h towards test termination. These differences, especially for the initial 2000 h, are believed to relate to reoxidation of the nickel anode at too high anode overpotential. Numerical simulation shows that for lower cell voltage (higher fuel utilisation), an increased anode area receives very little fuel [9]. Combined with air and steam back diffusion at the anode edge, also quantified by calculation [20], these zones are prone to reoxidation. Post mortem inspection often reveals an oxidised anode border (one to several millimeters wide, green NiO colour instead of grey Ni metal) on most tested stack cells. The previously mentioned improved cell design with modified sealing, better flow field and higher fuel conversion is expected to reduce this limitation.

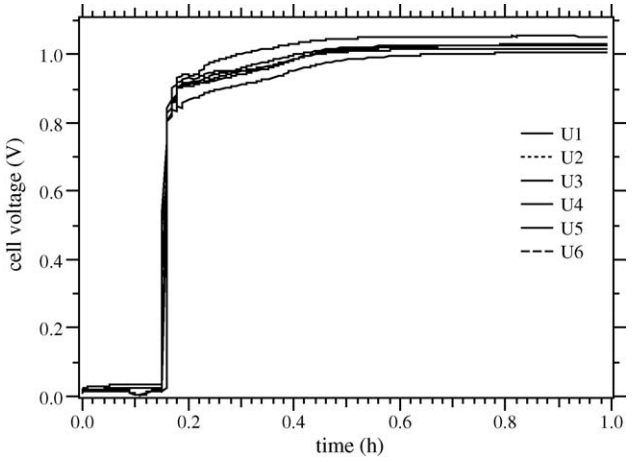

Fig. 13. Establishment of OCV on a 6-cell stack after fuel introduction, 750 °C.

3.5. Stack (100 W) operating cycle

A 6-cell stack of present HTceramix SOFCONNEX™ design and configuration (50 cm^2 cells with two feed holes; Fig. 10) was assembled to achieve 100 W_{el}. The next Figs. 13–18 describe the stack dynamics in test sequence.

Fig. 13 shows the moment of introduction of (dry) H_2 fuel to the anodes. All six cells respond quickly to equilibrate after 0.5 h above >1 V (stack voltage 6.16 V). H_2 flow was 8 ml min^{-1} cm^{-2} (2.4 L total), air flow 48 ml min^{-1} cm^{-2} (14.4 L total), corresponding to an excess ratio λ of 2.4.

Initial performance reached 82 W at 750 °C furnace temperature (790 °C for the highest locally measured temperature) under 25 A constant current polarisation. A brief excursion was made to 790 °C furnace temperature to reach 100 W_{el} at 28.5 A and 3.5 V stack voltage (0.585 V per cell). Fuel conversion at this stage was 53% and electrical efficiency 25%. The monitored temperature was maximally 830 °C at the H_2 excess outlet, while other temperatures measured within the stack showed local values below 800 °C.

Furnace temperature was returned to 750 °C and stack current to 25 A. Two identical stack *I–V* curves were recorded after 19 and 37 h of operation, plotted in Fig. 14. Stack power reached

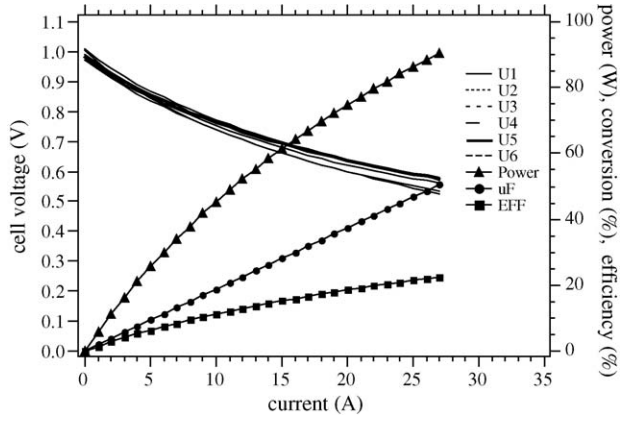

Fig. 14. *I–V–P* output of the 6-cell stack at 750 °C (furnace), real $T < 800$ °C, after 37 h of stable operation.

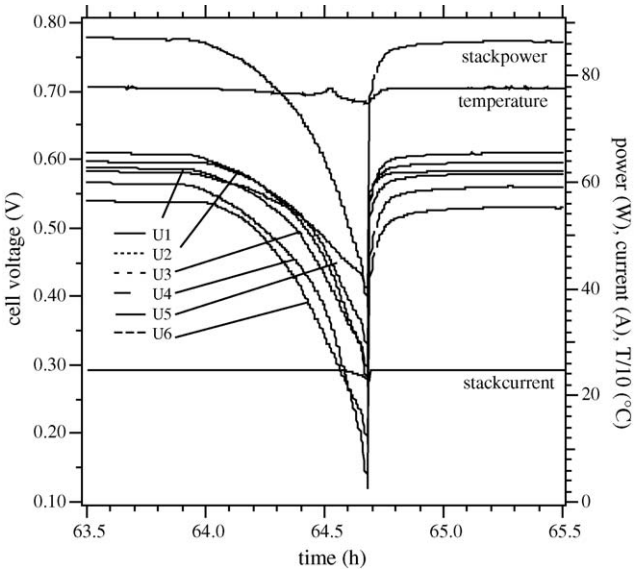

Fig. 15. Lack of H_2 supply (valve leak) under constant stack current (25 A), leading to severe cell voltage loss, restored to original values after reintroduction of H_2.

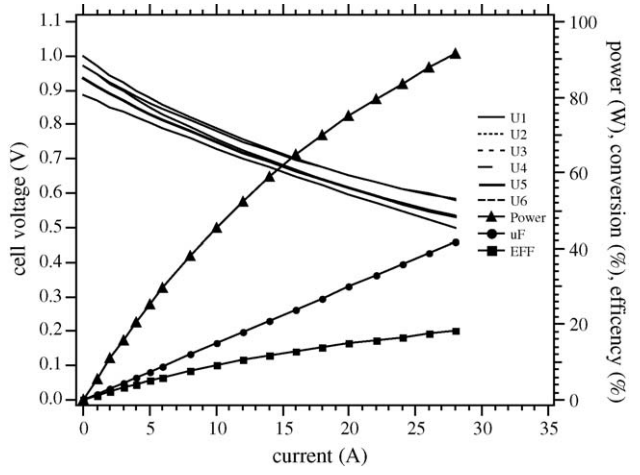

Fig. 16. *I–V–P* output of the 6-cell stack at 750 °C (furnace), real $T < 800$ °C, after 140 h of operation including a full thermal cycle and an unintended near-redox cycle (H_2 supply leak).

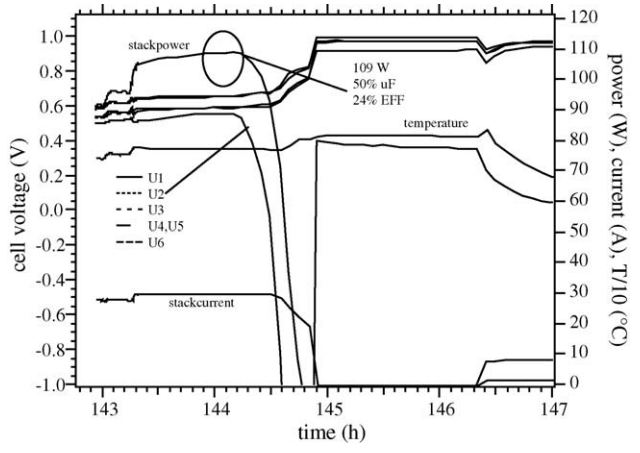

Fig. 17. Breakdown of cell number 2 during stack polarisation at 30 A, just after reaching peal power (109 W). End of stack test at 146 h.

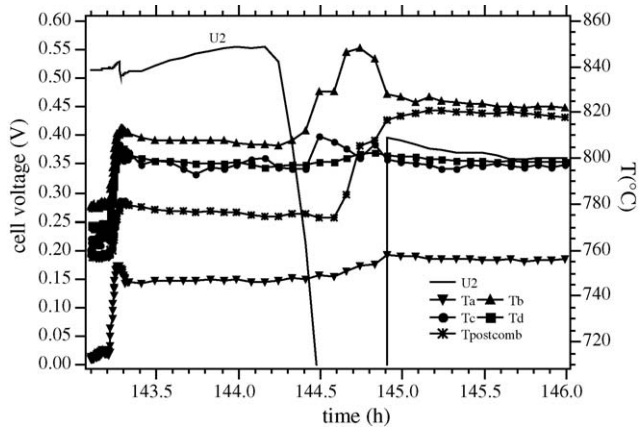

Fig. 18. Temperature at five locations near the stack, illustrating a spread of 70 K, during fracturing of cell number 2. One temperature (Tb) is seen to have risen substantially, pointing to a hot zone caused by H_2 leakage after the cell failure.

90 W at 27 A for an efficiency of 22% and fuel conversion of 50%. Cell performance homogeneity was adequate with an average value spread of 3.6% and OCVs of 1.01–1.05 V.

During the first 60 h, owing to cathode activation (Figs. 2A and 4), stack performance at constant polarisation increased from 82 to 87 W. At that moment, a severe H_2 leak occurred in the supply (due to a defect switching valve), while polarising the stack to 25 A, leading to cell voltage breakdown to 0.1–0.4 V (Fig. 15) during approximately 40 min. Switching to fresh H_2 supply restored the original performance: the stack therefore coped well with this involuntary simulation of a near-redox cycle.

The stack was subsequently taken through a full thermal cycle (800 °C → 50 °C → 800 °C). Upon renewed introduction of H_2 fuel at 750 °C, two out of the six cells (numbers 2 and 5) lagged behind in restoring to open circuit voltage. Their final OCV was only 0.88 and 0.93 V for a stack voltage of 5.7 V compared to 6 V before the thermal cycle. Some amount of damage incurred while cycling, whether redox or thermal.

Performance was again recorded after 140 h, including the H_2 leak incident and the thermal cycle (Fig. 16). A stack output of 90 W was reproduced, but at slightly higher H_2 flow (9 ml min^{-1} cm^{-2}) to compensate for lower OCVs. Hence, fuel conversion and electrical efficiency were lowered to 40 and 19%, respectively. Especially cell number 2 is seen to underperform, and value spread among the six cells has now increased to 9.2%.

Cell number 2 shortly later lead to stack failure, displayed in Fig. 17: at constant polarisation of 30 A and stable potentials of the five other cells, the potential of cell 2 steadily increased before collapsing, incidently at 0.5 V like in Fig. 1C. In Fig. 12 as well, during the first 500 h of operation, the performance is seen to strongly degrade when cell voltage is close to 0.5 V. The behaviour in Fig. 17 is believed to be related to anode limitation; around 0.5 V cell voltage, some poorly fed anode zones will be inactive (reoxidised), constricting the same substantial current to a smaller area, in turn leading to local heating, hot spot formation and crack initiation. Shortly before breakdown,

the stack reached peak power of 109 W_{el} (30 A, 3.62 V, fuel conversion 50%, efficiency 24%). After failure of cell number 2, the stack was cooled down. Fig. 18 displays the correlation between this failure and the temperature reading at various locations.

4. Conclusions

Transient and dynamic behaviour of short SOFC stacks (1–12 cells of 50 cm^2 each, and 5-cell stacks of 100 cm^2 per cell) were presented. Adequate power density is achieved with LSF cathodes, demonstrating performance activation and absence of any oscillations unlike cells with LSM cathodes, a phenomenon yet unexplained. Over 0.4 W cm^{-2} was achieved at 70% fuel conversion on a 1-cell stack (33 A) for a 450 h test without any degradation. In a 6-cell stack, power density reached 0.34 W cm^{-2} (100 W total) at 50% fuel conversion and 25% electrical efficiency. After severe gas leakage (supply fault) and a thermal cycle, this stack maintained its performance, until one cell (probably damaged during cycling) broke due to what appears to be crack initiation by local heating. Nevertheless, the results (>1 kW_{el} L^{-1}) are encouraging. Acceptable thermal cycling resistance was demonstrated. Long-term behaviour depends upon operating conditions (cell potential, fuel utilisation) and is yet insufficient (−5%/1000 h for a 5500 h test), though no metal interconnect protection measures have been implemented yet. Gas flow distribution over the cells is paramount, especially considering the risk of supporting anode edge reoxidation with strong implication for mechanical reliability. Modeling tools, in pair with experimental validation, are helping to design a new cell and stack configuration to alleviate the operating constraints.

Acknowledgements

Sincere thanks are due to Dr. K. Honegger (Sulzer Innotec, Switzerland) for stack testing (Figs. 7 and 8) and to the following funding agencies for financial support: Swiss Commission for Technology and Innovation (CTI contract 6649.3 IWS-IW), Swiss Federal Energy Office (OFEN project 43,428, contracts 86,895, 86,755, 100,457, 100,459), Swiss National Science Foundation (contract 200021/100721/1).

References

[1] R. Steinberger-Wilckens, L.G.J. de Haart, I.C. Vincke, L. Blum, A. Cramer, J. Remmel, G. Blass, F. Tietz, W.J. Quadakkers, Recent results of stack development at Forschungszentrum Juelich, in: S. Singhal, M. Dokiya (Eds.), Proceedings of the 8th International Symposium on Solid Oxide Fuel Cells, Electrochemical Society Proceedings Series, vol. 2003-07, Paris, The Electrochemical Society Inc., Pennington, New York, April 2003, p. 98.

[2] R. Barfod, S. Koch, Y.-L. Liu, P.H. Larsen, P.V. Hendriksen, Long term tests of DK-SOFC cells, in: S. Singhal, M. Dokiya (Eds.), Proceedings of the 8th International Symposium on Solid Oxide Fuel Cells, Electrochemical Society Proceedings Series, vol. 2003-07, Paris, The Electrochemical Society Inc., Pennington, New York, April 2003, p. 1158.

[3] H. Itoh, T. Yamamoto, M. Mori, T. Watanabe, T. Abe, Improved microstructure of Ni-YSZ cermet SOFC with long term stability, Denki Kagaku 64 (6) (1996) 549.

[4] A. Mitterdorfer, L.J. Gauckler, $La_2Zr_2O_7$ formation and oxygen reduction kinetics of the $La_{0.85}Sr_{0.15}Mn_yO_3$/$O_2$/YSZ system, Solid State Ionics 111 (1998) 185–218.

[5] K. Honegger, A. Plas, Evaluation of ferritic steel interconnects for SOFC stacks, in: H. Yokokawa, S. Singhal (Eds.), Proceedings of the 7th International Symposium on Solid Oxide Fuel Cells, Electrochemical Society Proceedings Series, vol. 2001-16, Tsukuba, Japan, The Electrochemical Society Inc., Pennington, New York, June 2001, p. 803.

[6] E. Batawi, A. Plas, W. Straub, K. Honegger, R. Diethelm, New cost-effective ceramic oxide phases used as protective coatings for Cr-based interconnects, in: S. Singhal, M. Dokiya (Eds.), Proceedings of the 6th International Symposium on Solid Oxide Fuel Cells, Electrochemical Society Proceedings Series, vol. 1999-19, Honolulu, Hawaii, The Electrochemical Society Inc., Pennington, New York, October 1999, p. 767.

[7] M. Molinelli, D. Larrain, R. Ihringer, L. Constantin, N. Autissier, O. Bucheli, D. Favrat, J. Van herle, Current collection and stacking of anode support cells with metal interconnects to compact repeating units, in: S. Singhal, M. Dokiya (Eds.), Proceedings of the 8th International Symposium on Solid Oxide Fuel Cells, Electrochemical Society Proceedings Series, vol. 2003-07, SOFC VIII, Paris, April 2003, pp. 905–913.

[8] L. Constantin, R. Ihringer, O. Bucheli, J. Van herle, Stability and performance of tape cast anode supported electrolyte cells, in: J. Huijsmans (Ed.), 5th European Solid Oxide Fuel Cell Symposium, Lucerne, Switzerland, July 2002, p. 132 (European Fuel Cell Forum Secretariat, Morgenacherstrasse 2F, CH-5452 Oberrohrdorf, Switzerland).

[9] N. Autissier, D. Larrain, J. Van herle, D. Favrat, CFD modeling tool for SOFC, J. Power Sources 131 (2004) 313–319.

[10] K. Honegger, R. Kruschwitz, M. Keller, G.M. Christie, Performance of SOFC stacks operated with CH_4 at reduced temperatures, in: S. Singhal, M. Dokiya (Eds.), Proceedings of the 6th International Symposium on Solid Oxide Fuel Cells, Electrochemical Society Proceedings Series, vol. 1999-19, Honolulu, Hawaii, The Electrochemical Society Inc., Pennington, New York, October 1999, p. 1019.

[11] J. Van herle, R. Ihringer, R. Vasquez, L. Constantin, O. Bucheli, Anode supported SOFC with screen-printed cathodes, J. Eur. Ceram. Soc. 21 (2001) 1855–1859.

[12] A.J. Bard, L.R. Faulkner, Electrochemical Methods, Fundamentals and Applications, John Wiley and Sons, 1980, p. 172.

[13] A. Hammouche, Contribution à l'étude de $LaSrMnO_3$ comme matériau d'électrode à oxygène à haute température, Ph.D. Thesis, National Polytechnic Institute of Grenoble, France, 1989, pp. 71, 76.

[14] J. Van herle, Oxygen reduction reaction mechanisms on SOFC cathodes, Ph.D. Thesis no. 1187, Federal Institute of Technology, Lausanne, Switzerland, 1993, p. 256.

[15] S. Widmer, Mécanismes de dépolarisation de la réduction de l'oxygène sur des interfaces structurées à haute température, Ph.D. Thesis no. 1732, Federal Institute of Technology, Lausanne, Switzerland, 1997, pp. 208–218.

[16] F. Ravussin, Caractérisations locales dans une pile à combustible SOFC, Diploma Thesis, LENI, Federal Institute of Technology (EPFL), Lausanne, Switzerland, March 2004.

[17] S.P. Simner, J.F. Bonnett, N.L. Canfield, K.D. Meinhardt, J.P. Shelton, V.L. Sprenkle, J.W. Stevenson, Development of lanthanum ferrite SOFC cathodes, J. Power Sources 113 (2003) 1–10.

[18] S. Simner, J. Stevenson, J. Bonnett, M. Anderson, Improved sinterability and performance of lanthanum ferrite SOFC cathodes, Fuel Cell Seminar (2003) 388–391.

[19] F.S. Baumann, J. Fleig, M. Konuma, U. Starke, H.-U. Habermeier, J. Maier, Strong performance improvement of $La_{0.6}Sr_{0.4}Co_{0.8}Fe_{0.2}O_3$ solid oxide fuel cell model cathodes by electrochemical activation, J. Electrochem. Soc. 152 (2005) A2074.

[20] D. Larrain, J. Van herle, F. Maréchal, D. Favrat, Generalized model of SOFC planar repeat element for design optimisation, J. Power Sources 131 (2004) 304–312.
[21] D. Larrain, J. Van herle, F. Maréchal, D. Favrat, Thermal modeling of a small anode supported solid oxide fuel cell, J. Power Sources 118 (2003) 367–374.
[22] D. Larrain, J. Van herle, D. Favrat, Modeling of cross-flow stack: sensitivity to thermal properties of the materials, in: S. Singhal, M. Dokiya (Eds.), Proceedings of the 8th International Symposium on Solid Oxide Fuel Cells, Electrochemical Society Proceedings Series, vol. 2003-07, Paris, The Electrochemical Society Inc., Pennington, New York, April 2003, p. 1478.